Available online at www.sciencedirect.com
ScienceDirect
Ceramics International 37 (2011) 1047–1053
CERAMICS INTERNATIONAL
www.elsevier.com/locate/ceramint

Densification and grain growth of 8YSZ containing NiO

R.M. Batista, E.N.S. Muccillo *

Energy and Nuclear Research Institute-CCTM, Av. Prof. Lineu Prestes, 2242, Cidade Universitária, S. Paulo 05508-000, SP, Brazil

Received 6 August 2010; received in revised form 20 September 2010; accepted 14 November 2010
Available online 28 December 2010

Abstract

The effects of NiO addition on sintering yttria-stabilized zirconia were systematically studied to understand the role of the additive in the sintering process of the solid electrolyte. Specimens of 8 mol% yttria-stabilized zirconia with NiO contents up to 5.0 mol% were prepared using different Ni precursors and sintered at several dwell temperatures and holding times. Densification and microstructural features were studied by apparent density measurements and scanning electron microscopy observations, respectively. The sintering dynamic study was carried out by following the linear shrinkage of powder compacts containing 0–0.75 mol% NiO. Small (up to 1.0 mol%) NiO addition was found to improve the sinterability of yttria-stabilized zirconia. The activation energy for volume diffusion decreases with increasing NiO content, whereas the grain boundary diffusion seems to be independent on this additive. The grain growth of yttria-stabilized zirconia is found to be enhanced even for small NiO contents.

Keywords: A. Sintering; A. Grain growth; Zirconia

1. Introduction

Yttria-stabilized zirconia (YSZ) has been the most studied material for application as solid electrolyte in high-temperature solid oxide fuel cells (SOFCs) [1]. For this application, the solid electrolyte must be impervious to the diffusion of molecular oxygen. This requirement imposes to the solid electrolyte a minimum relative density of ~93%. Commercial YSZ powders attain such high density after conventional sintering only at temperatures above 1350 °C [2,3]. Decrease of the sintering temperature could allow for simultaneous sintering (co-firing) of the solid electrolyte and the electrode components, thereby reducing the production cost of this device.

One approach to decrease the sintering temperature of materials consists in the addition of a sintering aid. Several ceramic additives have been investigated for that purpose. Transition metal oxides are favorite candidates to be used as sintering aids, because they have a relatively low melting temperature, allowing for densification by liquid phase mechanism. Nickel oxide, NiO, has a cubic crystalline structure and relatively high melting point (1984 °C) [4]. It is one of the preferred materials for anode component, usually the Ni/YSZ cermet. Few investigations may be found in the literature concerning the use of NiO as sintering aid for the YSZ solid electrolyte.

Decrease of sintered density of the cermet occurred with heavy NiO additions (40–60 wt.%) to zirconia–8 mol% yttria (8YSZ), although faster densification was obtained in the beginning of the sintering process [5]. van Herle and Vasquez [6] observed fast densification of 8YSZ with small (~1.5 mol%) NiO addition without any detriment of its properties. The grain growth of 10 mol% yttria-stabilized zirconia (10YSZ) was enhanced with NiO contents below the solubility limit, and decreased beyond that limit [7]. Recently, Zhang et al. [8] reported improved densification of 8YSZ with NiO additions.

None of the previous works studied the effect of NiO addition on the densification mechanisms of YSZ. For ceramic materials, sintering is the most important process to reach high densities with a desired microstructure. During sintering the surface energy of powder particles decreases according to several mass transport mechanisms [9]. Those mechanisms are usually thermally activated, and are predominant in specific temperature ranges, although overlapping among them is known to occur. The overall mechanisms occurring during sintering can be basically divided into those that promote decrease of the surface energy accompanied by densification of

* Corresponding author. Tel.: +55 11 31339203; fax: +55 11 31339276.
E-mail address: enavarro@usp.br (E.N.S. Muccillo).

0272-8842/$36.00
doi:10.1016/j.ceramint.2010.11.031

the ceramic material, and those that decrease the surface energy without any significant densification. The mechanisms responsible by most of densification during sintering of ceramics are grain boundary diffusion and volume diffusion. In general, grain boundary diffusion predominates in the initial stage of sintering, whereas volume diffusion plays a major role in the intermediate stage. Many theoretical models have been developed to predict the behavior of materials with sintering temperature and time [10–14]. The main purpose of this work is to perform a thorough investigation on the effect of NiO addition on densification behavior, grain growth and sintering dynamics of 8YSZ. Interpretation of experimental data was accomplished applying the model proposed by Wang and Raj [10], briefly described below.

1.1. Sintering model

In the Wang and Raj model [10] the linear shrinkage of a powder compact is related to the sintering temperature and time by:

$$-{}^{dL}/_{Ldt} = {}^{C\gamma V^{\frac{2}{3}} f(\rho)}/_{RTG^3} \cdot \exp\left(-{}^{Q}/_{k_B T}\right) + {}^{C\gamma V^{\frac{2}{3}} f_g(\rho)}/_{RTG^4} \cdot \exp\left(-{}^{Q_g}/_{k_B T}\right) \quad (1)$$

where C is a constant, V is the molar volume, γ is the surface energy, $f(\rho)$ is a function only of density, Q is the activation energy of the mechanism, k_B is the Boltzmann constant, T is the absolute temperature, L is the length of the material, R is the ideal gas constant, t is the time, G is the mean grain size, and the subscripts and g stand for volume diffusion and grain boundary diffusion, respectively. In the initial stage of sintering, Eq. (1) can be simplified to give:

$$-\frac{L_0}{L} \cdot \frac{d(\Delta L/L_0)}{dt} = \frac{C\gamma V^{2/3} f_g(\rho)}{eRTG^4} \cdot \exp\left(-\frac{Q_g}{k_B T}\right) \quad (2)$$

The activation energy for grain boundary diffusion can be obtained by further simplification of Eq. (2), resulting:

$$\ln\left(T \cdot \frac{L_0}{L} \cdot \frac{d(-\Delta L/L_0)}{dt}\right) = \frac{-Q_g}{k_B T} + \ln\left(C\gamma V^{2/3}\right) + \ln f_g(\rho) - 4 \cdot \ln\left(R^{1/4} G\right) \quad (3)$$

The second and the third terms on the right-side of Eq. (3) can be taken as constant during the initial stage of sintering, because the average grain size is approximately constant and the density changes only ~3% [9,10]. Then, the activation energy of the mechanism can be determined by plotting the left-side of Eq. (3) as a function of the reciprocal temperature.

Another useful approach is to analyze the variation of the temperature of maximum shrinkage. This can be done by a second derivation of Eq. (2) resulting:

$$-T_M^2 \cdot \frac{f'(\rho)}{f(\rho)} \cdot \frac{d\rho}{dT} = \frac{Q}{R} \quad (4)$$

Eqs. (3) and (4) were used in this work to analyze the effects of NiO additions on the activation energy of the mechanisms promoting the densification of the 8YSZ solid electrolyte.

2. Experimental

2.1. Powder materials and processing

Zirconia–8 mol% yttria (99.6%, Tosoh), NiO (99%, Alfa Aesar), $Ni(NO_3)_2{\cdot}6H_2O$ (99.9985%, Puratronic), $NiCO_3{\cdot}3Ni(OH)_2{\cdot}xH_2O$ (99.5%, Alfa Aesar) and $C_4H_6NiO_4{\cdot}4H_2O$ (99%, Caal) commercial powders were used as-received. NiO additions up to 5 mol% to 8YSZ were carried out by mechanical mixing.

For dilatometry experiments the starting materials were mixed together in the desired proportion in a mechanical mixer (Turbula, T2C model) for 1 h followed by calcination at 600 °C for 10 min. After deagglomeration of the powder mixtures, cylindrical compacts were prepared by uniaxial pressing in a 5 mm diameter stainless steel die followed by isostatic pressing (130 MPa).

Specimen preparation for other experiments were carried out by mixing and uniaxial pressing (60 MPa) followed by sintering in air at several dwell temperatures and holding times.

2.2. Characterization methods

Thermal decompositions of NiO precursor powders were analyzed by thermogravimetry, TG (Shimadzu, TGA 50) in stagnant atmosphere of synthetic air up to 1000 °C at a rate of 10 °C min^{-1}. Calcined mixtures were analyzed by X-ray diffraction (Bruker-AXS, D8 Advance) for phase characterization and to determine the mean crystallite size using the Scherrer equation. High-grade Si powder was used as external standard for instrumental error correction. X-ray diffraction analyses were performed between 28° and 88° 2θ range with 0.03° step size and 3 s counting time. Sintering dynamics was studied by dilatometry experiments (Setaram, Labsys model) in flowing synthetic air (40 mL min^{-1}) up to 1380 °C with heating rate of 8 °C min^{-1}. Densification of powder compacts was further studied by apparent density determination by measuring the sample mass and geometry. Selected pellets were observed in a scanning electron microscope (Philips, XL30) to determine the effects of NiO additions on the microstructure of the sintered solid electrolyte. The average grain size, G, of sintered specimens was calculated by the intercept method in a population of about 1000 grains.

3. Results and discussion

3.1. Powder characterization

Thermogravimetric curves of NiO precursors are shown in Fig. 1. The thermal decomposition of each precursor material is characterized by several steps of weight loss. These results are in general agreement with previous studies [15–18]. It is worth to note that the TG curve of nickel acetate exhibits a small

weight gain above ~518 °C. This effect was observed in experiments conducted under stagnant air atmosphere. The weight gain may be then associated to the oxidation of Ni residues, which are known to be formed during the decomposition reaction [18].

The thermogravimetric curve of trihydroxy nickel carbonate in the 500–1000 °C range shows a small weight loss of about 1%, whereas the decomposition reaction of nickel nitrate is complete up to ~400 °C.

Fig. 2 shows X-ray diffraction patterns of precursor materials after calcination at 600 °C for 10 min and that of 8YSZ powder. The abbreviations NO, NA, NC and NN are used to indicate the precursor material and stand for nickel oxide, nickel acetate, trihydroxy nickel carbonate and nickel nitrate, respectively. The phase characterization was carried out by comparison of the angular position and intensity of diffraction peaks with corresponding JCPDS files (71-1179 for NiO and 30-1468 for 8YSZ). All diffraction patterns of nickel oxide may be indexed according to that of NiO with a cubic NaCl-type structure. The space group and the mean crystallite size of calcined powders are shown in Table 1.

The crystallite size of 8YSZ agrees with that of the manufacturer specification. The crystallite size of NiO prepared from trihydroxy nickel carbonate is lower than that of 8YSZ, whereas the opposite trend occurs for other precursor materials. This result suggests that grain growth in specimens containing NiO may be dependent upon the precursor material.

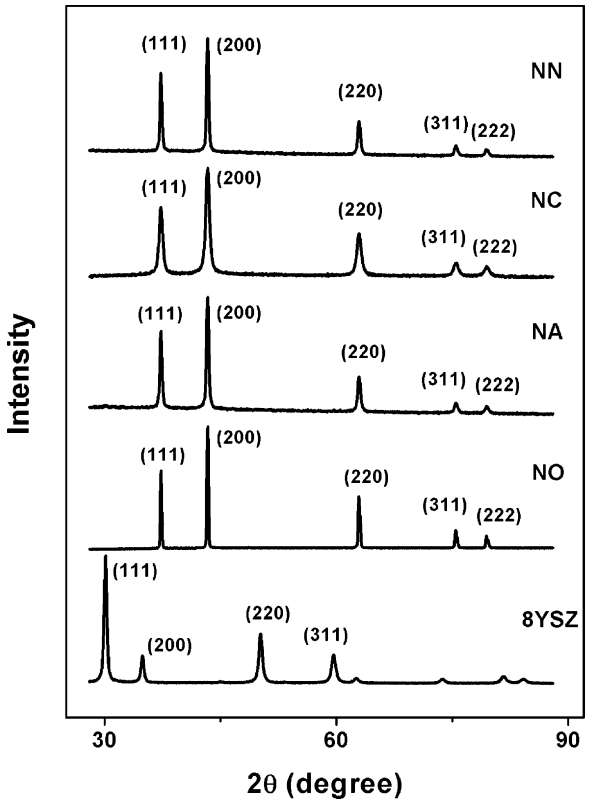

Fig. 2. X-ray diffraction patterns of starting materials calcined at 600 °C for 10 min.

3.2. Effect of NiO content on densification of 8YSZ

Linear shrinkage curves of powder compacts prepared with increasing amounts of trihydroxy nickel carbonate are shown in Fig. 3. This nickel oxide precursor was chosen for this study because of its relatively high purity, low crystallite size and low hygroscopic nature compared to nickel nitrate and nickel acetate. The onset temperature for shrinkage decreases with increasing NiO content. Moreover, densification is faster in specimens containing NiO. Total shrinkage at 1380 °C amounts 16.4% for 8YSZ and 19.9% for 8YSZ containing 0.75 mol% NiO. Table 2 shows values of total shrinkage, $(\Delta L/L_0)_{max}$, at 1380 °C for the studied specimens.

Table 1
Space group and mean crystallite size of 8YSZ and NiO prepared with several precursors calcined at 600 °C for 10 min.

	8YSZ	NiO (NA)	NiO (NN)	NiO (NO)	NiO (NC)
Space group	Fm3m	Fm3m	Fm3m	Fm3m	Fm3m
Mean crystallite size (nm)	25.6	46.4	50.6	251	21.5

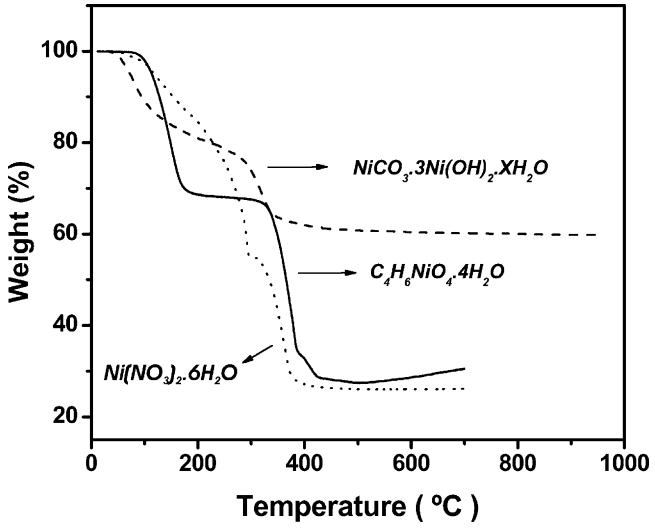

Fig. 1. Thermogravimetric curves of nickel-based precursor materials.

The derivative curves of the linear shrinkage of powder compacts are shown in Fig. 4. The temperature of maximum shrinkage, T_M, decreases with increasing NiO content. Values of T_M are listed in Table 2. For 8YSZ containing 0.75 mol% NiO T_M is approximately 75 °C lower than 8YSZ without the additive.

These results show that NiO additions below the solubility limit (~1.5 mol% at 1350 °C) increase the densification rate of 8YSZ. Complimentary results of densification were obtained by apparent density measurements of specimens prepared by conventional sintering. Results are given in terms of relative density. The theoretical density was calculated taking into account the mass and the volume of the unit cell. Unit cell volumes were determined from the lattice parameter for each

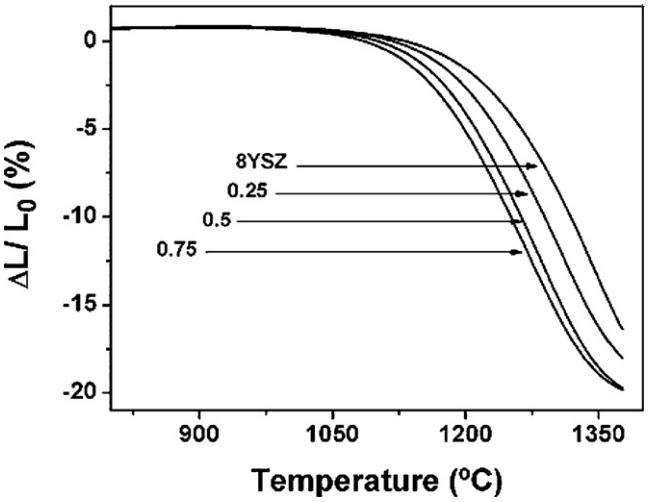

Fig. 3. Linear shrinkage curves of 8YSZ and 8YSZ with small NiO additions (mol%). Precursor material: trihydroxy nickel carbonate.

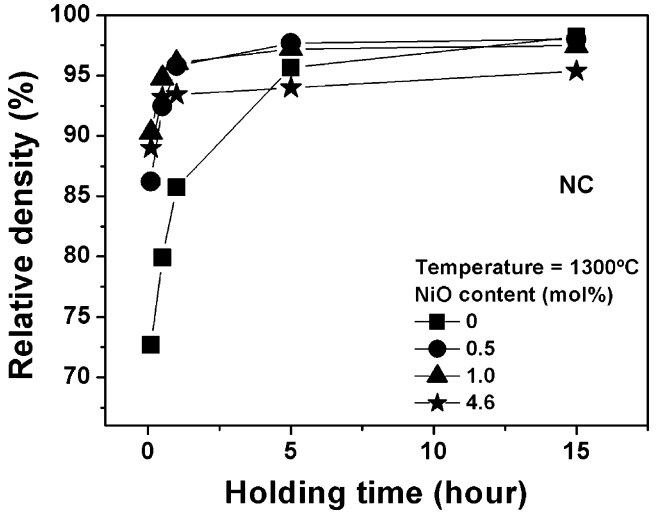

Fig. 5. Relative density versus holding time for 8YSZ and 8YSZ containing different amounts of NiO. Lines are only a guide to the eyes.

Table 2
Values of total shrinkage, $(\Delta L/L_0)_{max}$, at 1380 °C and temperature of maximum shrinkage, T_M, for 8YSZ and 8YSZ containing NiO specimens prepared with trihydroxy nickel carbonate precursor.

Specimen	$(\Delta L/L_0)_{max}$	T_M (°C)
8YSZ	16.4	1341
8YSZ + 0.25 NiO	18.0	1306
8YSZ + 0.50 NiO	19.7	1281
8YSZ + 0.75 NiO	19.9	1265

specimen and they are in agreement with values obtained by Kuzjukevics and Linderoth [19].

Fig. 5 shows the variation of relative density with holding time for specimens containing different amounts of NiO at a fixed temperature of 1300 °C. Specimens containing NiO show a fast increase in the relative density with short holding times compared to 8YSZ. Similar results were obtained for other sintering temperatures in the 1150–1350 °C range. The relative density of specimens containing 4.6 mol% NiO, that is above the solubility limit, is lower than that of 8YSZ for holding times higher than 5 h. This occurs because in these specimens two densification processes operate simultaneously, one for 8YSZ and other for NiO, and the densification kinetics of 8YSZ is faster than that of NiO [5].

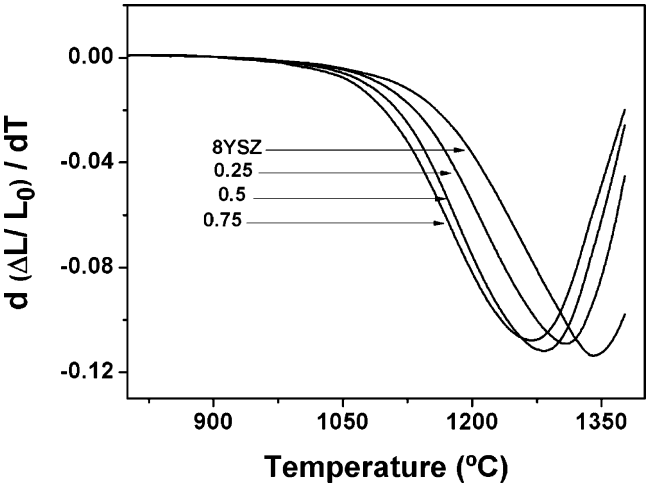

Fig. 4. Linear shrinkage rate curves of 8YSZ and 8YSZ with small NiO additions (mol%). Precursor material: trihydroxy nickel carbonate.

3.3. Effect of nickel precursor on densification

Fig. 6 shows linear shrinkage curves of 8YSZ powder compacts containing 0.5 mol% NiO prepared with different nickel oxide precursors. Except for compacts prepared with nickel acetate, these curves show a decrease in the onset temperature for shrinkage and an increase in the maximum shrinkage. Values of shrinkage at 1380 °C are listed in Table 3. The different behavior of the powder compact prepared with nickel acetate is probably related to the complex nature of the decomposition reaction of this precursor material with the surrounding atmosphere.

Derivative curves of linear shrinkage are shown in Fig. 7. These curves show that NiO addition to 8YSZ reduces the temperature for maximum shrinkage from ∼1340 to 1280 °C. The temperature of maximum shrinkage for different NiO precursors is listed in Table 3. It should be noted that T_M does not vary considerably with the nickel precursor, except for nickel acetate. Small differences in these temperatures may be attributed to residual impurities in the starting materials.

3.4. Effect of NiO on densification mechanisms

The effects of NiO additions on the densification mechanism of 8YSZ in the initial stage of sintering were studied by fitting experimental data obtained by dilatometry using Eq. (3). Fig. 8 shows, as an example, how regions of linear behavior were chosen for this analysis. In y-axes $a = dT/dt$ and $y = -\Delta L/L_0$. Data in these plots correspond to the specimen containing

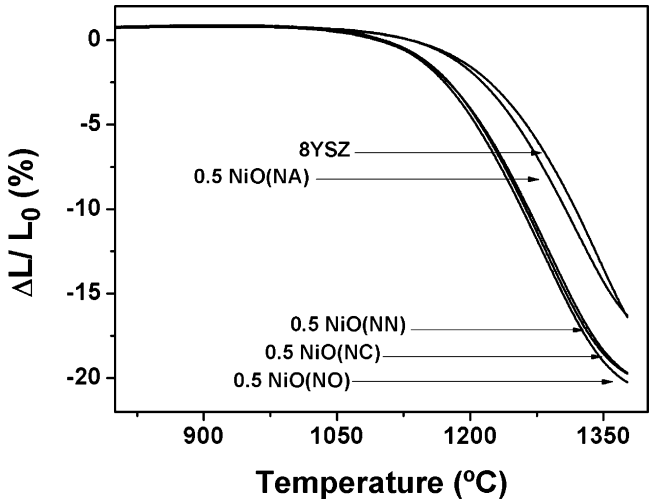

Fig. 6. Linear shrinkage curves of 8YSZ and 8YSZ with 0.5 mol% NiO obtained from different precursors.

Table 3
Values of total shrinkage, $(\Delta L/L_0)_{max}$, at 1380 °C and temperature of maximum shrinkage, T_M, for specimens containing 0.50 mol% NiO prepared with different nickel precursors.

Specimen	$(\Delta L/L_0)_{max}$	T_M (°C)
8YSZ	16.4	1341
8YSZ + 0.50 NiO (NA)	16.3	1318
8YSZ + 0.50 NiO (NC)	19.7	1281
8YSZ + 0.50 NiO (NO)	20.2	1280
8YSZ + 0.50 NiO (NN)	19.7	1287

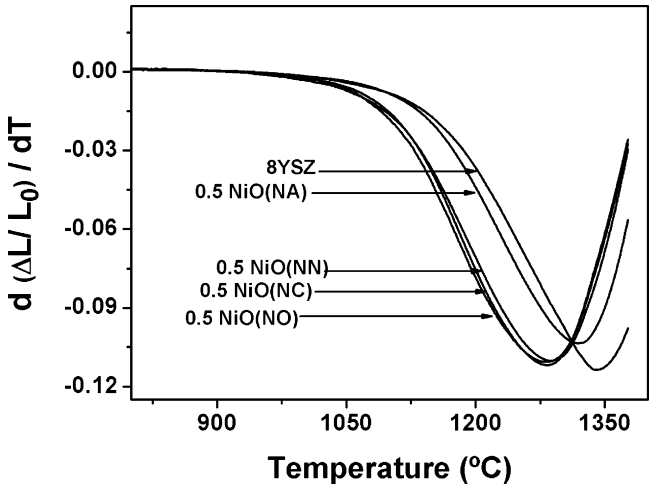

Fig. 7. Linear shrinkage rate curves of 8YSZ and 8YSZ with 0.5 mol% NiO obtained from different precursors.

0.25 mol% NiO prepared with trihydroxy nickel carbonate precursor. The linear range chosen is indicated by a parallel dotted line and refers to regions where both curves (corresponding to the left-side of Eq. (3) and its derivative) are linear. Similar treatment was carried out for experimental data obtained for other specimens. After fitting straight lines,

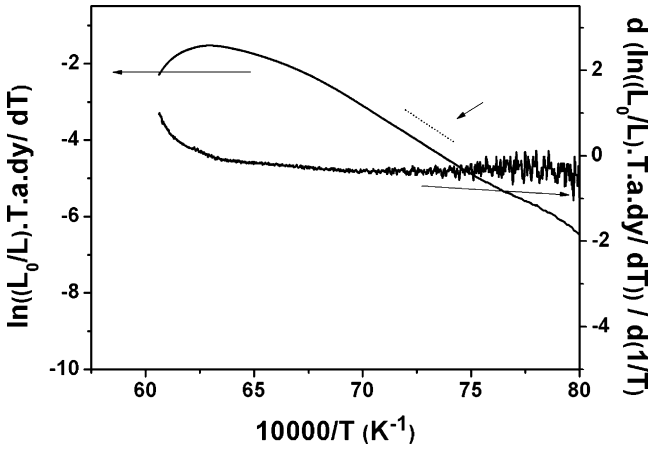

Fig. 8. Plots for the choice of the linear region for estimating grain boundary activation energy; specimen: 8YSZ + 0.25 mol% NiO (NC).

values for the grain boundary activation energy (Table 4) were estimated.

It is worth noting the similar values obtained for specimens without the additive (pure 8YSZ) and with 0.50 mol% NiO using nickel oxide as precursor material. Therefore, the densification mechanism by grain boundary diffusion is not influenced by small amounts of this additive. However, for specimens prepared with other NiO precursors, the grain boundary activation energy seems to be dependent on the decomposition behavior. For nickel nitrate, the decomposition reaction is complete up to 400 °C, and the activation energy is only slightly higher than that of 8YSZ. The trihydroxy nickel carbonate presented a continuous decomposition up to ∼1000 °C, and the grain boundary activation energy is, in this case, the highest. Then, these differences in the grain boundary activation energy may be explained as a result of the interaction of residues of the decomposition reaction with the diffusing species at the grain boundaries in the initial stage of sintering.

The overall results show improvement in the sinterability of 8YSZ with NiO additions. Moreover, analytical treatment of experimental data in the initial stage of sintering revealed that the densification mechanism by grain boundary diffusion is not influenced by the additive at levels below the solubility limit. The increase of sinterability is then expected to occur by volume diffusion. The activation energy for this mechanism may be correlated to the temperature for maximum shrinkage, T_M, through Eq. (4). Assuming that $f(\rho)$, in that equation, is

Table 4
Values of grain boundary activation energy for the studied specimens.

Specimen	E_{gb} (kJ mol^{-1})
8YSZ	267.5
8YSZ + 0.25 NiO (NC)	298.1
8YSZ + 0.50 NiO (NC)	315.0
8YSZ + 0.75 NiO (NC)	331.7
8YSZ + 0.50 NiO (NA)	285.0
8YSZ + 0.50 NiO (NN)	271.4
8YSZ + 0.50 NiO (NO)	267.4

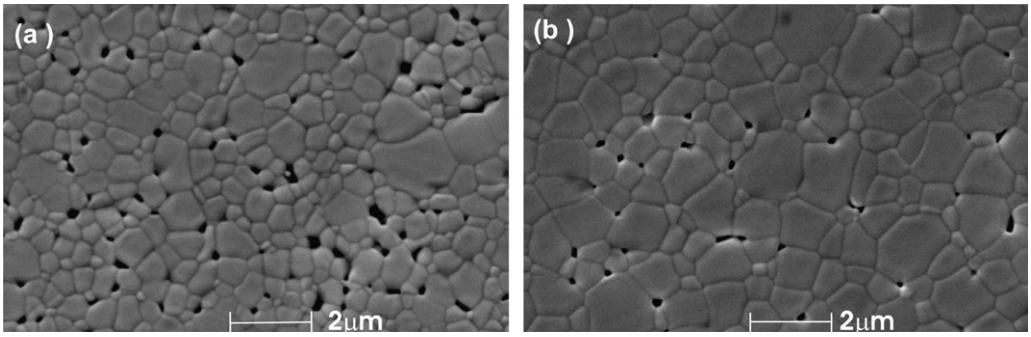

Fig. 9. Scanning electron microscopy micrographs of (a) 8YSZ and (b) 8YSZ containing 0.5 mol% NiO using trihydroxy nickel carbonate as precursor. Sintering conditions: 1350 °C for 0.5 h.

approximately constant for small NiO contents, the activation energy for volume diffusion decreases with decreasing T_M. Tables 2 and 3 show that T_M decreases for specimens containing NiO, independent on its content and precursor material, respectively. Therefore, NiO plays a major role in the volume diffusion mechanism during sintering of 8YSZ.

3.5. Effect of NiO on grain growth

Fig. 9 shows scanning electron microscopy micrographs of 8YSZ (Fig. 9a) and 8YSZ containing 0.5 mol% NiO (Fig. 9b) specimens sintered at 1350 °C for 0.5 h. It is known that NiO promotes an increase in the grain size of 8YSZ [5–7]. As can be seen in this figure, the grain growth process is enhanced even for small NiO contents.

Variation of the average grain size determined by the intercept method as a function of relative density is shown in Fig. 10 for selected specimens. The grain growth is accelerated for relative density values above ~95%, independent on the precursor material. Although the starting materials contain different impurities, these seem not to influence significantly the grain growth process. In addition, these results show that the crystallite size of NiO has negligible effect on grain growth. Specimens prepared with nickel oxide precursor (NO) exhibited slightly higher grain sizes compared to the ones prepared with trihydroxy nickel carbonate under the same sintering conditions. Then, the grain size/relative density ratio is nearly constant. In Fig. 10, specimens with higher grain size were sintered for longer holding times (>5 h) and a small decrease in the sintered density has probably occurred as a consequence of overfiring.

Fig. 11 shows a linear variation of the square of grain size with holding time. For short holding times no considerable variation of the grain size is observed. The change of slope of the linear fit evidences that grain growth is accelerated with increasing NiO content. From the slope of the linear fits, values for K, a temperature-dependent growth factor, were obtained. This growth factor is related to the grain boundary mobility, M_{gb}, by [20]:

$$K = 2\alpha M_{gb}\gamma_{gb} \tag{5}$$

where α is a geometrical constant dependent on the shape of the boundary, and γ_{gb} is the specific grain boundary energy (energy per unit area).

Fig. 12 shows the effect of NiO content on the growth factor for specimens prepared with trihydroxy nickel carbonate as

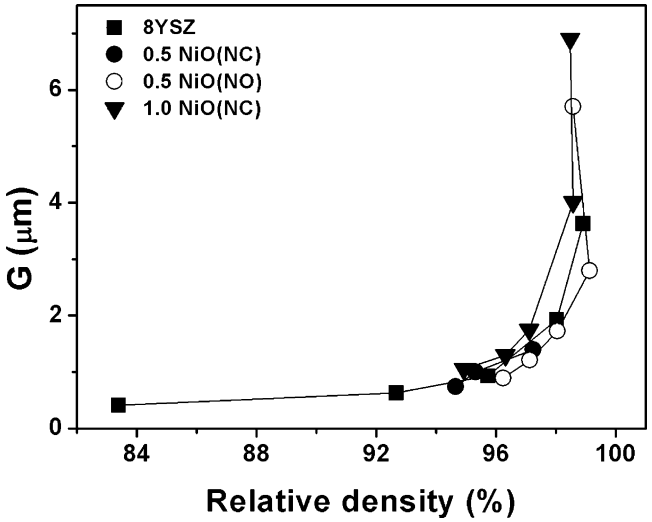

Fig. 10. Grain size versus relative density for 8YSZ and 8YSZ with NiO additive.

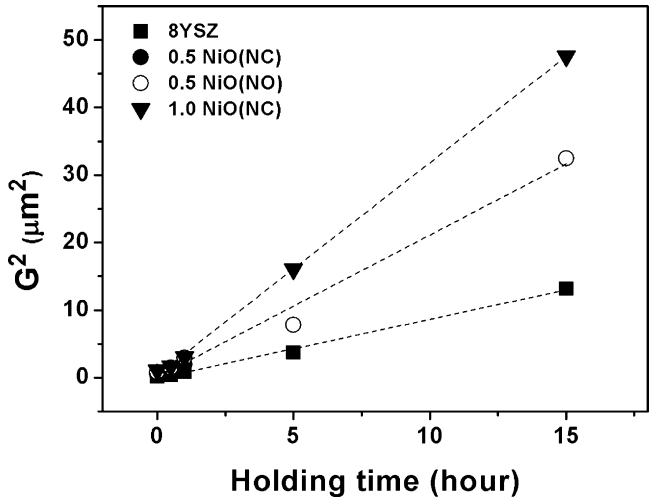

Fig. 11. Square of grain size versus holding time for 8YSZ and 8YSZ containing NiO.

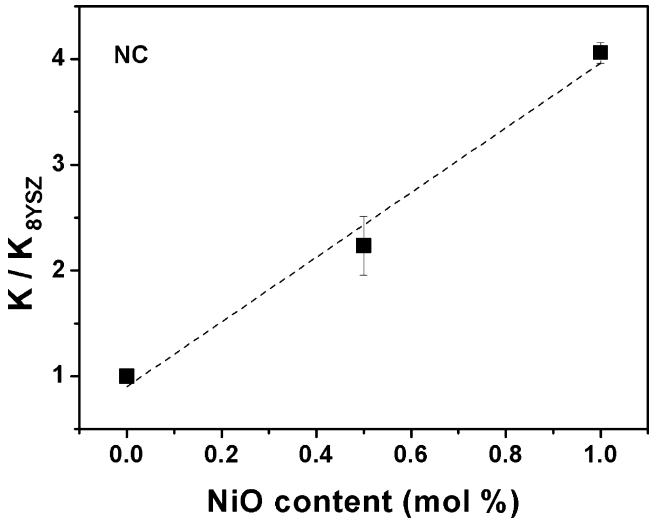

Fig. 12. Variation of the growth factor ratio with NiO content.

precursor at 1350 °C. In this case, the value of K was normalized to that of 8YSZ without the additive, K_{8ysz}, and shows a substantial increase with increasing NiO content.

4. Conclusions

Distinct effects were obtained with NiO additions to 8YSZ depending on its contents and nickel precursor. NiO increases the densification rate of 8YSZ for additions up to the solubility limit. The activation energy for grain boundary diffusion ($\sim$267 kJ mol^{-1}) remains constant with 0.5 mol% NiO addition, when the oxide precursor is used. Except for nickel acetate, volume diffusion is accelerated by small NiO amounts independent on the type of nickel precursor. The grain growth rate is enhanced by NiO addition to 8YSZ.

Acknowledgements

To FAPESP, CNEN and CNPq for financial support and to CCCH at IPEN for dilatometry experiments. One of the authors (R.M.B.) acknowledges FAPESP for the scholarship.

References

[1] J.W. Fergus, Electrolytes for solid oxide fuel cells, J. Power Sources 162 (2006) 30–40.
[2] I.R. Gibson, G.P. Dransfield, J.T.S. Irvine, Sinterability of commercial 8 mol% yttria-stabilized zirconia powders and the effect of sintered density on the ionic conductivity, J. Mater. Sci. 33 (1998) 4297–4305.
[3] de FlorioF D.Z., R. Muccillo, Sintering of zirconia–yttria ceramics studied by impedance spectroscopy, Solid State Ionics 123 (1999) 301–305.
[4] R.C. Weast, CRC Handbook of Chemistry and Physics, 64th ed., CRC Press Inc., Florida, 1983.
[5] T. Matsushima, H. Ohrui, T. Hirai, Effects of sinterability of YSZ powder and NiO content on characteristics of Ni-YSZ cermet, Solid State Ionics 111 (1998) 315–321.
[6] J. van Herle, R. Vasquez, Conductivity of Mn and Ni-doped stabilized zirconia electrolyte, J. Eur. Ceram. Soc. 24 (2004) 1177–1180.
[7] S. Chen, W. Deng, P. Sen, Stability of cubic ZrO_2 (10 mol.% Y_2O_3) when alloyed with NiO, Al_2O_3 or TiO_2: implications to solid electrolytes and cermets, Mater. Sci. Eng. B 22 (1994) 247–255.
[8] T.S. Zhang, Z.H. Du, S. Li, L.B. Kong, X.C. Song, J. Lu, J. Ma, Transitional metal-doped 8 mol% yttria-stabilized zirconia electrolytes, Solid State Ionics 180 (2009) 1311–1317.
[9] R.M. German, Sintering Theory Practice, John Wiley & Sons, New York, 1996
[10] J. Wang, R. Raj, Estimate of the activation energies for boundary diffusion from rate-controlled sintering of pure alumina, and alumina doped zirconia and titania, J. Am. Ceram. Soc. 73 (1990) 1172–1175.
[11] M.-Y. Chu, M.N. Rahaman, L.C. De Jonghe, R.J. Brook, Effect of heating hate on sintering and coarsening, J. Am. Ceram. Soc. 74 (1991) 1217–1225.
[12] J. Zhao, M.P. Harmer, Sintering kinetics for a model final-stage microstructure: a study in Al_2O_3, Philos. Mag. Lett. 63 (1991) 7–14.
[13] J.D. Hansen, R.P. Rusin, M.-H. Teng, D.L. Johnson, Combined-stage sintering model, J. Am. Ceram. Soc. 75 (1992) 1129–1135.
[14] D.L. Johnson, New method of obtaining volume, grain boundary, and surface diffusion coefficients from sintering data, J. Appl. Phys. 40 (1969) 192–200.
[15] S.A.A. Mansour, Spectroscopic and microscopic investigations of the thermal decomposition of nickel oxysalts. Part 1. Tetrahydroxy nickel carbonate, Thermochim. Acta 228 (1993) 155–171.
[16] N. Mizutani, M. Kato, H. Henmi, M. Mori, T. Hirayama, Influence of the self-generated and controlled atmosphere on the thermal decomposition of basic nickel carbonate, $NiCO_3{\cdot}2Ni(OH)_2{\cdot}4H_2O$, Thermochim. Acta 104 (1986) 101–109.
[17] S.A.A. Mansour, Spectroscopic and microscopic investigations of the thermal decomposition of nickel oxysalts. Part 2. Nickel nitrate hexahydrate, Termochim. Acta 228 (1993) 173–189.
[18] M.A. Mohamed, S.A. Halawy, M.M. Ebrahim, Non-isothermal decomposition of nickel acetate tetrahydrate, J. Anal. Appl. Pyrol. 27 (1993) 109–118.
[19] A. Kuzjukevics, S. Linderoth, Interaction of NiO with yttria-stabilized zirconia, Solid State Ionics 93 (1997) 255–261.
[20] M.N. Rahaman, Ceramic Processing Sintering, 2nd ed., CRC Press, Boca Raton, 2003.